Published in final edited form as:
J Urol. 2008 September ; 180(3): 1154–1160. doi:10.1016/j.juro.2008.04.140.

Histopathologic Assessment of Prostate Cancer Bone "Osteoblastic" Metastases

Martine P Roudier[1,*], **Colm Morrissey**[2,4], **Lawrence D True**[1], **Celestia S Higano**[3], **Robert L Vessella**[2,4], and **Susan M Ott**[5]

[1]Department of Pathology, University of Washington, Seattle WA.

[2]Department of Urology, University of Washington, Seattle, WA.

[3]Department of Medicine, Division of Oncology, University of Washington, Seattle, WA.

[4]Research Service, VA Puget Health Sciences Center, Seattle, Washington.

[5]Department of Medicine Division of Endocrinology, University of Washington, Seattle WA.

Abstract

Purpose—Many patients with prostate cancer develop bone metastases that appear osteoblastic on radiographs, yet these patients have an elevated risk of fractures. The discrepancy between the radiological and clinical aspects of those events is not well understood. The purpose of this study was to better characterize the histopathology of bone processes in prostate cancer bone metastases.

Materials and Methods—Histomorphometry was used to evaluate multi-site bone biopsies in each of 12 patients who died with multiple bone metastases, 7 of whom had received bisphosphonate therapy.

Results—Bone histomorphometry revealed a wide spectrum of cancer-induced bone changes in different metastatic sites within individual patients, ranging from a pronounced osteodense to a pronounced osteopenic type. Each metastatic lesion was associated with various amounts of resorption. Decreased bone volume was seen in half of all biopsies. Osteodense lesions were largely composed of undermineralized woven bone, which increases frailty of the new bone. Interestingly, woven bone was produced by alkaline phosphatase spindle-shaped cells arising from the connective stroma surrounding tumor cells. Bone response generally was similar in both bisphosphonate-treated patients and those who did not receive bisphosphonate therapy.

Conclusions—Despite the osteoblastic nature of bone metastases in prostate cancer, the osteolytic-osteopenic bone lesions found in each clinically osteoblastic patient may explain the frequent fractures observed in these patients. In addition, the finding that woven bone formed directly from the tumor stroma and not from the adjacent bone surface supports further research into the mechanisms of abnormal bone formation in prostate cancer bone metastases.

Keywords

Prostatic neoplasms; bone; neoplasm metastasis; diphosphonates; histology

[*]Present address for correspondence and reprint requests: Martine Roudier, MD, PhD, Department of Pathology, Amgen Washington, 1201 Amgen Court West, Seattle, WA 98119-3105, Phone: 206-265-8120, Fax: 206-265-6459, E-mail: mroudier@amgen.com.

INTRODUCTION

With an estimated 186,320 new cases and 28,660 deaths in 2008 in the United States, prostate carcinoma is one of the most common cancers in older men in Western countries. Despite an initial response to androgen deprivation therapy, patients with progressive prostate cancer often develop multiple bone metastases. In contrast with metastases caused by other carcinomas such as breast, thyroid, kidney, and lung that destroy bone and are termed “osteolytic,” prostate cancer generally causes a bone-forming or “osteoblastic” response. Osteoblastic bone metastases in prostate cancer appear on plain radiographs as areas of increased density (osteodense lesions) and on bone scans as hot spots of increased bone formation.[1] In addition, serum bone alkaline phosphatase levels[2], 3 and iliac bone histomorphometry[4–6] studies have confirmed that bone formation is increased in the tumor-involved sites. However, although these are osteoblastic lesions, the bone that is produced in response to the tumor cells may be fragile and abnormal.

On the other hand, radiographs, iliac bone histomorphometry, and markers of bone turnover indicate that osteolysis is also commonly associated with the prostate metastases, even when the predominant pattern appears to be osteoblastic.[4–6] The localization and ratio of osteolytic versus osteoblastic areas in patients with prostate cancer have not been documented.

Clinically, patients with prostate cancer often present with bone loss and increased risk of fracture due to an aging skeleton and/or prostate-derived systemic factors.[7] The underlying abnormalities in bone metabolism could influence the skeletal response to prostate cancer metastases. The pathophysiology of prostate cancer bone metastasis is complex and likely involves many different causal factors and pathways, the principal of which have not yet been identified.[8] To better understand the pathophysiology of prostate cancer bone metastases, we examined a set of 20 different bone biopsies in each of 12 autopsied patients and performed histomorphometry assessments of each bone specimen.

MATERIALS AND METHODS

Patient Clinical Data and Bone Biopsies

Twelve patients at the University of Washington Medical Center were enrolled in a previously described IRB-approved rapid autopsy program between 1998 and 2001.[9] These autopsies were performed within 2 to 4 hours of death and specimens were acquired from 20 pre-determined anatomic bone sites. Duplicate bone biopsies were obtained using a 1.2-cm diameter trephine from iliac crests, sacral wings, proximal epiphysis of humerus and femur, vertebrae L1 to L5 and T8 to T12, the anterior aspect of the 7th rib, and the sternum. Any grossly visible rib metastases were also obtained.

Bone Histomorphometry

One set of the duplicate biopsies was fixed in 10% buffered formalin for 48 hours. Samples were then dehydrated with graded ethanol and embedded in methylmethacrylate.[10] Sections were cut at 7 microns using a Jung K microtome with tungsten carbide tip blade and stained with Goldner’s trichrome. Tartrate-resistant acid phosphatase (TRAP) staining was performed using pararosanilin and naphtol MX. Alkaline phosphatase staining was performed using nitro blue tetrazolium/5-bromo-4-chloro-3-indolyl phosphate (NBT/BCIP) or naphtol AS-MX phosphate.[11]

Histomorphometric measurements of cancellous bone used a semi-automated technique with a side-arm attachment to the microscope and a digitizing tablet from which surfaces and

areas can be manually drawn and computed (Osteomeasure, Osteometrics Inc. Decatur, GA). Measurements were made on a randomly chosen 15-contiguous-square area in cancellous bone at 10x magnification. The measurements were expressed according to the recommendations of the American Society of Bone and Mineral Research[12] and included the following: bone volume; osteoid surface; osteoblast number; osteoid thickness; osteoid volume; eroded surface; and osteoclast surface. Based on normative bone histomorphometry data for males aged between 40 to 80 years,13 a biopsy was defined as osteodense if total bone volume was >35% and osteopenic if total bone volume was <18%. Normal eroded bone surface was assumed to be <2.3%. Additional measurements made were as follows:

- Osteoclast number: TRAP specific staining was performed on serial sections. Osteoclasts with TRAP activity were counted on the previously measured surface.
- Lamellar bone volume: the proportion of tissue volume occupied by lamellar bone was measured as observed using a light microscope with polarization.
- Woven bone volume: calculated by subtracting lamellar bone volume from total bone volume.
- Tumor volume: the proportion of tissue volume occupied by tumor tissue.

Statistical Analysis

Correlation analyses were performed using the statistical analysis package PRISM TM version 2.0 (GraphPad). Spotfire software (Spotfire DecisionSite) was used for histomorphometry data analysis. Comparative statistical tests were not performed.

RESULTS

Clinical Data

We studied the bone specimens of 12 men who died of advanced prostate cancer with bone metastases. Relevant clinical data are presented in Table 1. Of the 12 patients with bone metastases at autopsy, 11 had osteoblastic lesions on bone scan or X-ray surveys. The median age at the time of death was 67 years (range: 47 to 83 years). All patients were white. The median survival after diagnosis was 5 years (range: 1 to 11 years). The median time interval from diagnosis to androgen independence was 3.5 years (range: 0 to 8 years), and the median survival after androgen independence was 2.5 years (range: 1 to 6 years). All patients had been previously treated with androgen ablation therapy. The median duration of androgen ablation therapy was 3.5 years (range: 1.5 to 11 years). The median terminal serum prostate-specific antigen (PSA) level was 548 ng/ml (range: 24 to 7402 ng/ml). Nine patients were subsequently treated with chemotherapy when androgen therapy failed. Ten patients received palliative radiation therapy at sites of bone metastasis.

Seven patients were treated with bisphosphonates, either pamidronate (n=5; 90 mg i.v. every 4 weeks) or zoledronic acid (n=2; 4 mg i.v. every 4 weeks), with treatment duration ranging from 5 to 21 months. The bisphosphonate treatment was initiated after development of androgen independent bone metastases. The time between necropsy and the last dose of bisphosphonate treatment ranged from 1 week to 3.5 months.

Bone samples analyzed

Of the 240 bone biopsy samples obtained, 139 samples were either >50% necrotic (n=82, mainly in patients receiving radiation therapy to the spine) or were tumor-free (n=57). The remaining 101 samples were included in the histomorphometric analyses. One patient did not have tumor on any study sample. However, since a paraffin-embedded bone biopsy

adjacent to one of his study samples did contain tumor, that sample was included in the histomorphometric analyses but excluded from summary statistics.

Qualitative findings

No patient had lesions with characteristics that were entirely either osteolytic or osteoblastic. One patient with 20 tumor-containing biopsies had no significant uptake on repeated bone scans and minimal bony reaction in response to the presence of tumor cells.[1] In the remaining 81 bone metastases from 10 patients, half of the tumors were predominantly osteodense and the rest were predominantly osteopenic. Surprisingly, in each patient there was a spectrum of bone lesions from osteodense to osteopenic that occurred randomly within different bone sites, without histological changes in the carcinoma (Fig. 1A–B). This mixed pattern of osteodense and osteopenic was even observed in a single biopsy (Fig. 1C).

In osteodense bone specimens, an osteoblastic reaction to the tumor cells consisted mostly of woven bone, with small amounts of osteoid and inclusions of native bone trabeculae appearing as lamellar bone. These inclusions varied in size from one biopsy to another (Fig. 2A–D). In some cases an intact lamellar trabecular network remained, with woven bone around the edges of the normal bone. In contrast, in osteopenic biopsies, which might have been interpreted as osteolytic on X-rays, the woven bone was found in areas where there was a total loss of preexisting lamellar bone (Fig. 1B).

Woven bone and osteoid were mainly observed arising from the tumor stroma located within the bone marrow cavity (Fig. 2A, B). Progressive stages of woven bone formation were observed (Fig. 2A–C), culminating in a lacy network of bone within the marrow space between the native trabecular bone (Fig. 2C). To a lesser extent, appositional new woven bone was also observed along the native trabecular bone. Viewed with polarization, some woven bone was observed in all tumor-involved metastases (Fig. 2D).

Interestingly, well-differentiated osteoblasts, defined as cuboidal cells with basophilic cytoplasm lining osteoid, were rarely observed on the woven bone. Instead, spindle-shaped cells, or flat cells, were seen lining woven osteoid and entrapped as osteocytes in the woven bone. Early osteoblastic lesions consisted of a network of fibroblast-type and/or stromal cells, osteoid, and capillaries supporting the tumor stroma (Fig. 3A and B). These fibroblast-like cells were alkaline phosphatase positive, indicating their osteoblast lineage (Fig. 3C). Rarely, well differentiated osteoblasts were observed in areas of bone repair secondary to sites of tumor and bone necrosis. Osteoclasts were observed in the usual focal pattern, either on the surface of woven or lamellar bone or osteoid, and rarely in the tumor stroma without contact to bone.

Quantitative histomorphometry data in biopsies containing tumor

In the 102 biopsies which contained metastatic lesions (including one that was adjacent to a metastatic lesion), the areas and surfaces were quantitated. A similar total tissue area of 24 mm^2 was measured in each biopsy. Results are shown in Figure 4 and Table 2.

Tissue volume contains bone marrow, tumor, fat cells, vasculature, and bone. The bone, in turn, is composed of woven bone, lamellar bone, and osteoid. Tumor volume was a median of 39% of total volume, with a maximum of 88% in the osteopenic bone biopsies.

The median total bone volume was 24% (mean, 29%) of the tissue volume, with a range of 3.7% to 74% (Fig. 4A). An osteodense pattern (defined as bone volume > 35%) was observed in 34 biopsies (33% biopsies) and an osteopenic pattern (defined as bone volume < 18%) was observed in 43 biopsies (42% biopsies).

The amount of normal bone in the metastases was also examined. When only the volume of normal lamellar bone per total tissue volume was considered, 96 (94%) of bone biopsies were osteopenic (lamellar bone volume/tissue volume range: 4% to 14%, median: 9%) indicating the extent of the osteolytic process and resulting bone loss (Fig. 4B). In these biopsies, the total bone volume is composed of lamellar bone, woven bone, or osteoid. The median values (and range) as a percentage of tissue volume were: lamellar 7.5% (0.0%–57%), woven 15% (3%–70%), and osteoid 1% (0.014%–5.8%) (Fig. 4B–D).

The eroded surface included either osteoid, woven bone, or lamellar bone. Typically around 1.9% in normative data,[13] it was >2.4% for 64 biopsies (63%) and greater than 10% in nearly one-fifth (18%) of all biopsies, suggesting an intense, continuously lytic process associated with the osteoblastic process. The maximum eroded surface seen in the analyzed biopsies was 40% (Fig. 4E). Osteoclasts in tumor biopsies ranged from 0 to 20 (Fig. 4F).

Histomorphometry data in biopsies from sites without tumor

In 12 non-tumor-bearing bone biopsies from various sites that were additionally studied from this cohort (one biopsy from each patient), bone volume/tissue volume ranged from 8% to 19%, with a mean of 12%; this finding is indicative of generalized skeletal frailty. Neither osteoid nor woven bone was found in these biopsies. The eroded surface was 3% of total bone surface, indicating bone loss and slightly increased bone resorption compared to normative data for an age-matched population.

Histomorphometry data in bisphosphonate-treated patients

Osteoclasts from bisphosphonate-treated patients were either absent (3 patients), or when present (3 patients) they appeared as larger, multinucleated, unstained or faintly TRAP-stained cells (Fig. 5A). In contrast, osteoclasts in tumor biopsies from non–bisphosphonate-treated patients were smaller and stained intensely with TRAP (Fig. 5B).

When osteoclast number per bone surface (Fig. 6E) and TRAP-positive osteoclasts from bisphosphonate-treated patients (Fig. 6F) were compared to non–bisphosphonate-treated patients, there was a non-significant increased number of osteoclasts per bone surface and a non-significant decrease in the number of TRAP-positive osteoclasts in bisphosphonate-treated patients. This was explained by a good correlation (r^2=0.794) between the number of TRAP-positive osteoclasts observed in bisphosphonate-treated patients and time of bisphosphonate therapy interruption before biopsy, indicating a relapse of the osteolysis process when bisphosphonates were interrupted, however briefly, in these patients. There was no statistical difference between the 2 groups in bone volume, woven bone volume, osteoid volume, and eroded surface, indicating that bisphosphonates do not appear to modify the overall architecture of bone in prostate cancer bone metastasis.

DISCUSSION

Prostate cancer bone metastases are usually defined as osteoblastic on radiographs. However, among patients with various types of bone metastases—prostate cancer, non-small cell lung cancer, breast cancer, and multiple myeloma—prostate cancer patients had the highest NTX levels, a urine marker of bone turnover.14 In this study, the histomorphometric changes of bone provide a basis for these findings. Histomorphometric analysis of 101 metastatic biopsies showed a tremendous heterogeneity of lesions. We found an overall average bone volume of 29%, which is slightly increased compared to a normal age-matched bone volume (18–24%) and confirms the overall osteoblastic process.[13] However, despite an increase in average bone volume, approximately half of the 101 biopsies were osteopenic and half were osteodense. In addition, this heterogeneity of bone changes was

reproduced within individual patients, with a spectrum of lesions from osteopenic to osteodense, indicating a low bone mass in half of the bone metastases that were sampled in each patient. This may contribute to the histologic frailty observed in the skeleton of these patients, even in dense metastatic lesions. The heterogeneous phenomenon was randomly distributed throughout the skeleton and included metastatic biopsies with normal to high bone volume (18% to 35%), osteodense bone volume (>35%), and osteopenic bone volume (<18%).13 We were not able to determine how old each metastatic lesion was in this study, so we could not tell if some of the variability was due to lesions of different ages.

Within each of the 3 volume categories (osteodense, normal, and osteopenic), bone biopsies varied in remodeling types as follows: osteodense bone without resorption (a pure osteoblastic pattern), osteodense bone with osteolysis (a mixed pattern), osteopenic bone with high resorption (a pure osteolytic pattern), and osteopenic bone with production of woven bone (a mixed pattern). The variable association of bone formation and bone resorption with independent bone volumes suggests that bone turnover is totally uncoupled and independent of residual bone mass in prostate cancer bone metastasis.

In addition to the osteopenic status of half of the metastatic biopsies, most of the formed bone was woven bone, even in hyperdense lesions. Woven bone is observed in growing young bones and usually is only associated in adult life with pathologic conditions such as fracture repair, where the rate of bone resorption is high and fracture callus is made of woven bone matrix that is incompletely mineralized.[15] Woven bone in this study was mostly produced by spindle-shaped cells that were alkaline-phosphatase positive, indicating an osteoblastic lineage. Our observation suggests that woven bone production in patients with prostate cancer bone metastases might result from reproduction of primitive bone, production of immature osteoblastic cells, and/or inhibition of bone-producing cells by tumor cell factors. Immature osteoblasts have been found to be associated with an increase in the ratio of receptor activator of NF-κB ligand (RANKL) to osteoprotegerin (OPG) in the bone milieu.[16, 17] This altered ratio is expected to result in concomitantly increased osteolytic activity in predominantly osteoblastic diseases and might thus contribute to the clinical complications resulting from prostate cancer bone metastases.

It was interesting to note that the new bone was formed in the marrow spaces and not adjacent to the bone surface. Normal bone remodeling always occurs on the bone surface, with osteoclastic resorption preceding osteoblast formation. This study demonstrates that in this pathological condition bone may be formed de novo in the marrow without the requirement for pre-existing bone resorption. As expected, eroded surface area was greater than normative values,[13] both in tumor-bearing biopsies (as high as 40%) and in non-tumor-bearing biopsies, suggesting a local and systemic bone response secondary to tumor-associated circulating factors, androgen ablation, and stresses associated with the events that contributed to the patient's death. This finding further emphasizes the general frailty of the normal skeleton in prostate cancer patients with bone metastases.

While bone resorption markers generally increase during the aging process, androgen therapy induces additional bone loss and factors produced by tumor cells in bone increase osteolysis dramatically.[8] Bisphosphonates are used to impede the osteoclastic degradation of bone in these patients at any stage of bone disease.[18] Surprisingly, in our study the number of osteoclasts increased in bisphosphonate-treated biopsies. In addition, fewer of those osteoclasts were acid-phosphatase positive, which might represent a stage of recovery or indicate decreased activity due to bisphosphonate treatment. Recently, findings of irregular osteoclasts have been reported in patients with postmenopausal osteoporosis treated with aminobisphosphonates.[19, 20] The bone microenvironment might respond by trying to recruit more osteoclasts, while not actually affecting osteoclast activity. However, this study was

limited by the fact that the biopsies were taken at the termination of the disease and represented only a snapshot of prostate cancer bone metastases.

CONCLUSIONS

In summary, this study suggests that prostate cancer induces mixed bone responses, with both osteolytic and osteoblastic areas within the same biopsy. Furthermore heterogeneity of bone histomorphometry is seen within the same patient. While it is known that patients with metastatic prostate cancer to the bone sustain fractures and that elevated urinary N-telopeptide levels indicate significant bone resorption, this study provides an anatomical explanation for these clinical findings. In addition, osteoblastic lesions are composed of increased abnormal woven bone, formed in marrow spaces from the tumor stroma and not from the bone surface. This abnormal woven bone is formed by fibroblast-like cells that express alkaline phosphatase and thus are from osteoblastic lineage. These findings should change our understanding of the “osteoblastic” process in prostate cancer. Future research into the reduction of abnormal bone formation in patients with prostate cancer could benefit from an increased focus on targeted therapies that act on osteoclast activity, as well as factors that alter the normal differentiation and proliferation of osteoblasts and osteoclasts.

Acknowledgments

We thank the patients and their families who consented to the research autopsy program and allowed us to perform this study. We acknowledge Julie Hahn for excellent technical work and Carsten Goessl for critical reading of the manuscript. Amy Foreman-Wykert, Geoffery Smith, and Jonathan Latham provided editorial assistance.

Funding Sources: This work was supported in part by an OBRIEN award from the NIDDK (P50 DK 47656-08), an NCI Program Project Grant (P50 DK47656-10), an NIH Prostate Cancer SPORE (NCI 1P50CA97186-01), the Departments of Veterans Affairs and Defense, the Richard M Lucas Foundation, and the Prostate Cancer Foundation.

REFERENCES

1. Roudier MP, Vesselle H, True LD, Higano CS, Ott SM, King SH, et al. Bone histology at autopsy and matched bone scintigraphy findings in patients with hormone refractory prostate cancer: the effect of bisphosphonate therapy on bone scintigraphy results. Clinical and Experimental Metastasis 2003;20:171. [PubMed: 12705638]
2. Wymenga LF, Groenier K, Schuurman J, Boomsma JH, Elferink RO, Mensink HJ. Pretreatment levels of urinary deoxypyridinoline as a potential marker in patients with prostate cancer with or without bone metastasis. BJU International 2001;88:231. [PubMed: 11488735]
3. Plebani M, Bernardi D, Zaninotto M, De Paoli M, Secchiero S, Sciacovelli L. New and traditional serum markers of bone metabolism in the detection of skeletal metastases. Clinical Biochemistry 1996;29:67. [PubMed: 8929827]
4. Berruti A, Dogliotti L, Gorzegno G, Torta M, Tampellini M, Tucci M, et al. Differential patterns of bone turnover in relation to bone pain and disease extent in bone in cancer patients with skeletal metastases. Clinical Chemistry 1999;45:1240. see comment. [PubMed: 10430790]
5. Clarke NW, McClure J, George NJ. Morphometric evidence for bone resorption and replacement in prostate cancer. British Journal of Urology 1991;68:74. [PubMed: 1873694]
6. Garnero P, Buchs N, Zekri J, Rizzoli R, Coleman RE, Delmas PD. Markers of bone turnover for the management of patients with bone metastases from prostate cancer. British Journal of Cancer 2000;82:858. [PubMed: 10732759]
7. Eastham JA. Bone health in men receiving androgen deprivation therapy for prostate cancer. J Urol 2007;177:17. [PubMed: 17161994]
8. Vessella RL, Corey E. Targeting factors involved in bone remodeling as treatment strategies in prostate cancer bone metastasis. Clin Cancer Res 2006;12:6285s. [PubMed: 17062715]

9. Roudier MP, True LD, Higano CS, Vesselle H, Ellis W, Lange P, et al. Phenotypic heterogeneity of end-stage prostate carcinoma metastatic to bone. Human Pathology 2003;34:646. [PubMed: 12874759]

10. Lebeau A, Muthmann H, Sendelhofert A, Diebold J, Lohrs U. Histochemistry and immunohistochemistry on bone marrow biopsies. A rapid procedure for methyl methacrylate embedding. Pathology, Research and Practice 1995;191:121.

11. Liu C, Sanghvi R, Burnell JM, Howard GA. Simultaneous demonstration of bone alkaline and acid phosphatase activities in plastic-embedded sections and differential inhibition of the activities. Histochemistry 1987;86:559. [PubMed: 3610670]

12. Parfitt AM, Drezner MK, Glorieux FH, Kanis JA, Malluche H, Meunier PJ, et al. Bone histomorphometry: standardization of nomenclature, symbols, and units. Report of the ASBMR Histomorphometry Nomenclature Committee. Journal of Bone and Mineral Research 1987;2:595. [PubMed: 3455637]

13. Compston, J. Histomorphometric manifestations of age-related bone loss. In: Rosen, CJ.; Glowacki, J.; Bilezikian, JP., editors. The Aging Skeleton. 1st ed.. San Diego, CA: Academic Press; 1999. p. 251-262.

14. Coleman RE, Major P, Lipton A, Brown JE, Lee KA, Smith M, et al. Predictive value of bone resorption and formation markers in cancer patients with bone metastases receiving the bisphosphonate zoledronic acid. J Clin Oncol 2005;23:4925. [PubMed: 15983391]

15. Mulder L, Koolstra JH, den Toonder JM, van Eijden TM. Relationship between tissue stiffness and degree of mineralization of developing trabecular bone. J Biomed Mater Res A 2008;84:508. [PubMed: 17618500]

16. Atkins GJ, Kostakis P, Pan B, Farrugia A, Gronthos S, Evdokiou A, et al. RANKL expression is related to the differentiation state of human osteoblasts. Journal of Bone and Mineral Research 2003;18:1088. [PubMed: 12817763]

17. Thomas GP, Baker SU, Eisman JA, Gardiner EM. Changing RANKL/OPG mRNA expression in differentiating murine primary osteoblasts. Journal of Endocrinology 2001;170:451. [PubMed: 11479141]

18. Smith MR, Eastham J, Gleason DM, Shasha D, Tchekmedyian S, Zinner N. Randomized controlled trial of zoledronic acid to prevent bone loss in men receiving androgen deprivation therapy for nonmetastatic prostate cancer. J Urol 2003;169:2008. [PubMed: 12771706]

19. Weinstein RS, Chambers TM, Hogan EA, Webb WW, Wicker CA, Manolagas SC. Giant osteoclast formation after long-term oral aminobisphosphonate therapy for postmentopausal osteoporosis. Journal of Bone and Mineral Research 2007;22 suppl 1:S17.

20. Dempster DW, Zhou H, Nieves JW, Barbuto N, Cosman F, Lindsay R. Unusual osteoclast morphology in teriparatide-treated patients who have been pretreated with alendronate. Journal of Bone and Mineral Research 2007;22 suppl 1:S29.

ABBREVIATIONS

TRAP Tartrate-resistant acid phosphatase

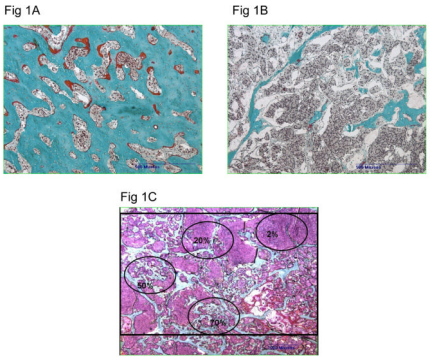

Fig. 1.

Spectrum of histological patterns observed in prostate cancer bone metastases from one patient: (A) Osteodense biopsy and (B) osteopenic biopsy taken from two different anatomical sites in the same patient. In all biopsies, bone marrow is entirely filled with prostate cancer cells. Magnification 5x. (C) Low magnification (1.25x) of a metastatic biopsy showing heterogeneity of bone volumes and remodeling types within a single biopsy; bone is green, prostate cancer is pink, and osteoid is red. The black rectangle on the photograph represents the area measured in each biopsy and corresponds to 15 consecutive fields in the image analysis system. Note the difference between approximative bone volumes indicated in the 5 black ovals drawn over the photograph. Goldner's-Masson-Trichrome stain.

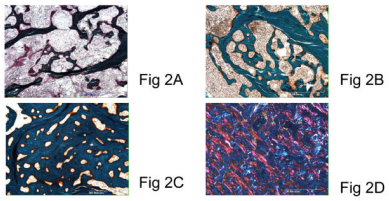

Fig. 2.

Photomicrographs of tumor-bearing bone biopsies showing progression of the osteodense/osteoblastic pattern of prostate cancer bone metastases. (A) Tumor bearing lesion with early irregular tumor-induced bone trabeculae arising from the tumor-infiltrated bone marrow space and bridging normal-looking native bone trabeculae. Note the osteolysis of native trabeculae. (B) Thickening of tumor-induced irregular bone trabeculae. Network of large tumor-induced trabeculae with small remains of barely visible native bone trabeculae. Note association of a large osteolytic pattern remodeling native and new bone trabeculae. (C) Osteodense osteoblastic pattern consisting of thick new bone trabeculae filling most of the bone marrow space, note the persistence of one native bone trabeculae and the absence of lytic component. Goldner's-Masson-Trichrome stain. Magnification 5x. (D) Aspect of a large osteodense tumor-bearing biopsy (same as shown in Fig1A) observed with polarization. The dense bone formed between the native trabeculae network was totally woven bone without lamellar bone. Goldner's-Masson-Trichome stain. Magnification 5x.

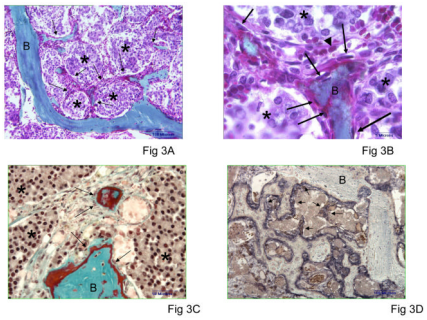

Fig 3A Fig 3B

Fig 3C Fig 3D

Fig. 3.

Formation of tumor-induced bone in prostate cancer bone metastases (undecalcified sections). (A) Early new bone formation arising from tumor stroma (arrows). Lamellar bone and new bone are blue/green (letter B). The bone formation arises from stroma walls of the tumor (tumor is marked by an asterix). Goldner's-Masson-Trichrome stain. Magnification 20x. (B) Higher magnification of Fig 3A showing detail of spindle-shaped cells (arrows) close to osteoid and capillary (short arrow). Goldner's-Masson-Trichrome stain. Magnification 40x. (C) Spindle cells (arrows) forming woven bone are alkaline phosphatase positive (black); NBT/BCIP. Magnification 20x.

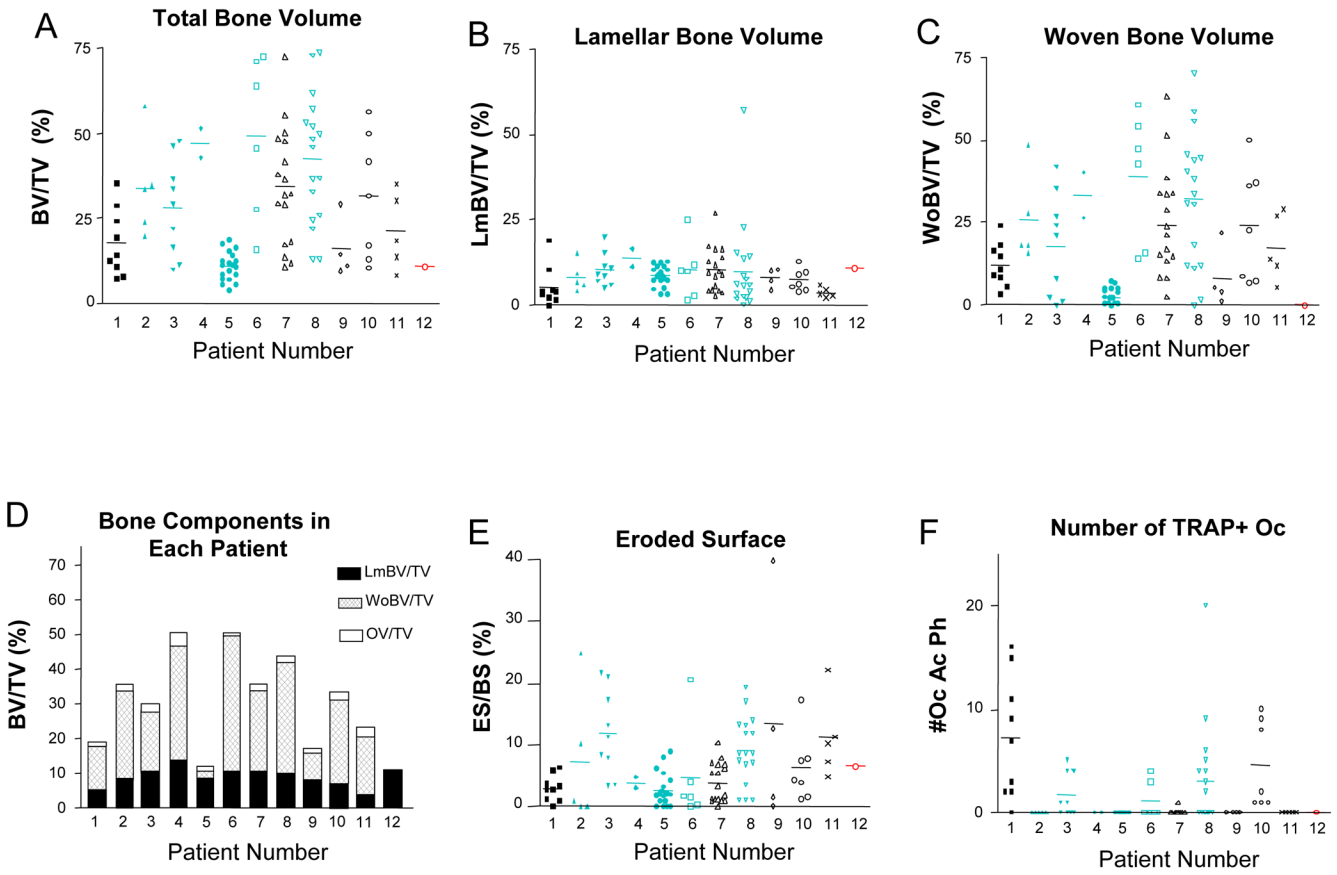

Fig. 4.

Histomorphometric measurements of biopsies from the 12 patients: (A) bone volume/tissue volume; (B) lamellar bone volume/tissue volume (LmBV); (C) woven bone volume/tissue bone volume (WoBV/TV); (D) percentage of bone components in each patient: lamellar bone in dark green (LmBV/TV), woven bone in light green (WoBV/TV), and osteoid bone volume in orange (OV/TV); (E) eroded surface/bone surface; and (F) osteoclast number. Patients indicated in blue were treated with bisphosphonates. Patient 12 had only non tumor-bearing biopsies; data from one non-tumor bearing biopsy are displayed. Bars represent median values.

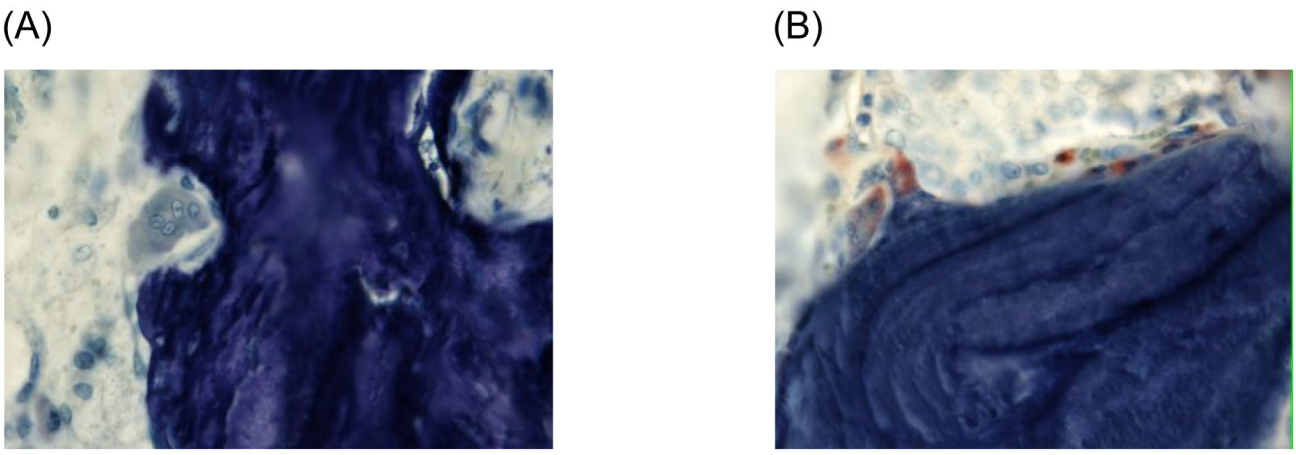

Fig. 5.
TRAP-positive osteoclasts in bone metastases. TRAP-toluidine blue staining. Magnification 10x. (A) Bisphosphonate-treated patients; TRAP-positive osteoclasts are large and pale. (B) Non–bisphosphonate-treated patients; TRAP-positive osteoclasts are small and bright red.

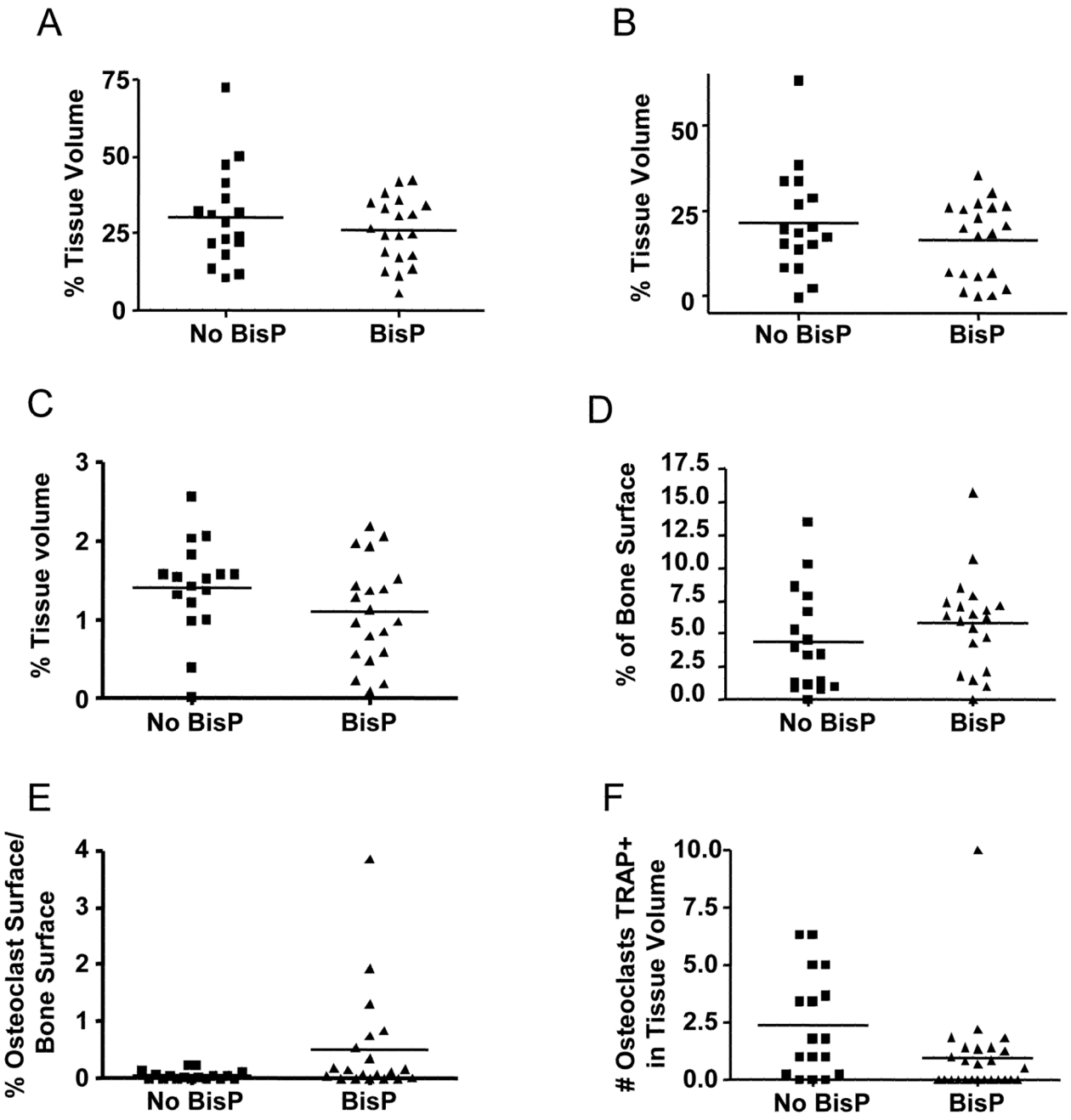

Fig. 6.

Comparison of (A) bone volume/tissue volume, (B) woven bone volume/tissue volume, (C) osteoid volume/tissue volume, (D) eroded surface/bone surface, (E) osteoclast surface/bone surface, and (F) osteoclast number in bisphosphonate-treated and non–bisphosphonate-treated patients. There was no significant difference between any of the bone criteria.

Table 1

Baseline Demographics and Disease Characteristics

Variable	All Patients (n = 12)
Age at death (years), median (range)	67 (47–83)
Years since diagnosis, median (range)	5 (1–11)
Years since bone metastasis diagnosis, median (range)	3 (0–5)
Terminal serum PSA (ng/ml), median (range)	548 (24–7402)
Androgen ablation therapy	
Received androgen ablation therapy	12 (100)
Years to androgen independence, median (range)	3.5 (0–8)
Years of treatment, median (range)	3.5 (1.5–11)
Bisphosphonate treatment	
Received pamidronate, n (%)	5 (42)
Received zoledronate, n (%)	2 (17)
Months of treatment[a], median (range)	13 (5–21)
Months from last dose to death[a], median (range)	2 (0.2–3.2)
Chemotherapy used by >2 patients, n(%)[b]	
Mitoxantrone	7 (58)
Docetaxel	5 (42)
Estramustine	5 (42)
Gemcitabine	5 (42)
Cisplatin	3 (25)
Carboplatin	3 (25)
No chemotherapy	3 (25)
Radiation location[c], n(%)	
Spine	5 (42)
Hip	4 (33)
Pelvis	2 (17)
Sacrum	2 (17)
Femur	1 (8)
No radiation	2 (17)
Corticosteroid[d], n (%)	
Dexamethasone	6 (50)
Prednisone	4 (33)
No corticosteroid	3 (25)

[a] Among the 7 patients who received a bisphosphonate

[b] Seven patients received combination chemotherapy

[c] Three patients had radiation therapy at >1 location

[d] One patient received both dexamethasone and prednisone.

Table 2

Histomorphometric Data for 101 Tumor-Containing Samples from 11 Patients

Bone Criteria	Median (range)
Bone volume/tissue volume (%)	24 (3.7–74)
Lamellar bone volume/tissue volume (%)	7.5 (0.0–57)
Woven bone volume/tissue volume (%)	15 (3.0–70)
Osteoid volume/total volume (%)	1.0 (0.014–5.8)
Osteoblast surface/bone surface (%)	0.37 (0.0–10)
Eroded surface/bone surface (%)	4.1 (0.0–40)
Osteoclast surface/bone surface (%)	0.2 (0.0–18)
No. of TRAP-positive osteoclasts	0.0 (0.0–20)
Tumor volume/total volume (%)	39 (0.0–88)

TRAP = tartrate-resistant acid phosphatase.